Observation of the semileptonic decays $D^0 \to K_S^0 \pi^- \pi^0 e^+ \nu_e$ and $D^+ \to K_S^0 \pi^+ \pi^- e^+ \nu_e$

The BESIII collaboration

E-mail: besiii-publications@ihep.ac.cn

ABSTRACT: By analyzing e^+e^- annihilation data corresponding to an integrated luminosity of $2.93\,\text{fb}^{-1}$ collected at a center-of-mass energy of $3.773\,\text{GeV}$ with the BESIII detector, the first observation of the semileptonic decays $D^0 \to K_S^0 \pi^- \pi^0 e^+ \nu_e$ and $D^+ \to K_S^0 \pi^+ \pi^- e^+ \nu_e$ is reported. In the hypothesis that all events correspond to $K_1(1270)$ decays, the branching fractions are measured to be $\mathcal{B}(D^0 \to K_1(1270)^- (\to K_S^0 \pi^- \pi^0) e^+ \nu_e) = (1.69^{+0.53}_{-0.46} \pm 0.15) \times 10^{-4}$ and $\mathcal{B}(D^+ \to \bar{K}_1(1270)^0 (\to K_S^0 \pi^+ \pi^-) e^+ \nu_e) = (1.47^{+0.45}_{-0.40} \pm 0.14) \times 10^{-4}$ with statistical significance of 5.4σ and 5.6σ, respectively. When combined with measurements of the $K_1(1270) \to K^+ \pi^- \pi$ decays, the absolute branching fractions are determined to be $\mathcal{B}(D^0 \to K_1(1270)^- e^+ \nu_e) = (1.08^{+0.14+0.08}_{-0.13-0.10} \pm 0.21) \times 10^{-3}$ and $\mathcal{B}(D^+ \to \bar{K}_1(1270)^0 e^+ \nu_e) = (1.70^{+0.26}_{-0.23} \pm 0.13 \pm 0.35) \times 10^{-3}$. The first and second uncertainties are statistical and systematic, respectively, and the third uncertainties originate from the assumed branching fractions of the $K_1(1270) \to K\pi\pi$ decays.

Contents

1 Introduction

Semileptonic charm decays induced by the $c \to se^+\nu_e$ process are dominated by pseudoscalar (K) and vector ($K^*(892)$) mesons, i.e. contain a kaon and at most one pion in the final-state hadronic systems [1, 2]. Semileptonic decays with higher multiplicity final states involving a kaon and two pions are highly suppressed and are expected to be mostly mediated by the axial-kaon system with a mixing angle θ_{K_1} [3]. Thus knowledge of θ_{K_1} is essential for theoretical calculations describing the decays of D particles into strange axial-vector mesons [4–6]. The $D \to \bar{K}\pi\pi e^+\nu_e$ decays provide a unique opportunity to study $K_1(1270)$ and $K_1(1400)$ mesons in a clean environment, without any additional hadrons in the final states. Such studies can lead to a better determination of θ_{K_1} as well as of the masses and widths of the K_1 mesons, which currently all have large uncertainties [7]. By exploiting the measured properties of $D \to \bar{K}_1(1270)\ell^+\nu_\ell$ and $B \to K_1(1270)\gamma$ decays, the photon polarization in $b \to s\gamma$ can be determined without considerable theoretical ambiguity, according to refs. [8, 9].

The BESIII collaboration, performing studies of the hadronic systems $K^-\pi^+\pi^-$ and $K^-\pi^+\pi^0$, reported the first observation of semileptonic D decays involving a $K_1(1270)$ [10, 11], and measured the branching fractions (BFs) $\mathcal{B}(D^0 \to K_1(1270)^- e^+\nu_e) = (1.06 \pm 0.12^{+0.09}_{-0.15} \pm 0.21) \times 10^{-3}$ and $\mathcal{B}(D^+ \to \bar{K}_1(1270)^0 e^+\nu_e) = (2.30 \pm 0.26^{+0.18}_{-0.22} \pm 0.50) \times 10^{-3}$. Here the first and second uncertainties are statistical and systematic, respectively, and the third uncertainties originate from the assumed BFs of $K_1(1270)^{0,+} \to K^+\pi^-\pi^{0,+}$ [7]. The decays $D^0 \to K_S^0\pi^-\pi^0 e^+\nu_e$ and $D^+ \to K_S^0\pi^+\pi^- e^+\nu_e$ have not yet been observed. In 2011, based on the $K^+\pi^+\pi^-$ system in the decay of $B^+ \to J/\psi K^+\pi^+\pi^-$, the Belle collaboration found the BFs of $K_1(1270) \to K\rho, K\omega$, and $K^*(892)\pi$ to be consistent with previous measurements, but reported the measured BF of $K_1(1270) \to K_0^*(1430)\pi$ to be significantly smaller [12]. Furthermore, measurements of the BF ratio $R_{K_1(1270)} = \frac{\mathcal{B}_{K_1(1270) \to K^*\pi}}{\mathcal{B}_{K_1(1270) \to K\rho}}$ yield different results

depending on the decay channels used [13–17], whereas they are expected to be identical under the narrow width approximation for the $K_1(1270)$ meson assuming CP conservation in strong decays [18]. Measurements of the BFs of $D \to K_1(1270)(\to K_S^0 \pi \pi)e^+\nu_e$ decays are desirable, as they would improve the knowledge of the relative decay rates of $K_1(1270)$ into final states with one kaon and two pions.

This paper presents the first observation of the semileptonic decays $D^0 \to K_S^0\pi^-\pi^0 e^+\nu_e$ and $D^+ \to K_S^0\pi^+\pi^- e^+\nu_e$ and measurements of the BFs of $D^0 \to K_1(1270)^- e^+\nu_e$ and $D^+ \to \bar{K}_1(1270)^0 e^+\nu_e$. The analysed data samples come from e^+e^- collisions at a center-of-mass energy of $3.773\,\mathrm{GeV}$, which were collected by the BESIII detector operating at the BEPCII storage ring. These samples correspond to an integrated luminosity of $2.93\,\mathrm{fb}^{-1}$ accumulated at the $\psi(3770)$ resonance [19]. Throughout this paper, charge conjugate channels are always implied.

2 Detector and data sets

The BESIII detector [20] records e^+e^- collisions provided by the BEPCII storage ring [21] in the center-of-mass energy range from 2.0 to $4.95\,\mathrm{GeV}$, with a peak luminosity of $1 \times 10^{33}\,\mathrm{cm}^{-2}\,\mathrm{s}^{-1}$ achieved at $\sqrt{s} = 3.773\,\mathrm{GeV}$. BESIII has collected large data samples in this energy region [22]. The cylindrical core of the BESIII detector covers 93% of the full solid angle and consists of a helium-based multilayer drift chamber (MDC), a plastic scintillator time-of-flight system (TOF), and a CsI(Tl) electromagnetic calorimeter (EMC), which are all enclosed in a superconducting solenoidal magnet providing a $1.0\,\mathrm{T}$ magnetic field. The solenoid is supported by an octagonal flux-return yoke with resistive-plate-counter muon-identification modules interleaved with steel. The charged-particle momentum resolution at $1\,\mathrm{GeV}/c$ is 0.5%, and the $\mathrm{d}E/\mathrm{d}x$ resolution is 6% for electrons from Bhabha scattering. The EMC measures photon energies with a resolution of 2.5% (5%) at $1\,\mathrm{GeV}$ in the barrel (end-cap) region. The time resolution in the TOF barrel region is $68\,\mathrm{ps}$, while that in the end-cap region is $110\,\mathrm{ps}$. Details about the design and performance of the BESIII detector are given in ref. [20].

Monte Carlo (MC) simulated data samples produced with a GEANT4-based [23] software package, which includes the geometric description of the BESIII detector and the detector response [24], are used to determine detection efficiencies and to estimate background contributions. The simulation models the beam-energy spread and initial-state radiation (ISR) in the e^+e^- annihilation with the generator KKMC [25, 26]. An 'inclusive' MC event sample includes the production of $D\bar{D}$ pairs (including quantum coherence for the neutral D channels), the non-$D\bar{D}$ decays of the $\psi(3770)$, the ISR production of the J/ψ and $\psi(3686)$ states, and the continuum processes incorporated in KKMC [25, 26]. All particle decays are modeled with EVTGEN [27, 28] using BFs either taken from the Particle Data Group (PDG) [7], when available, or otherwise estimated with LUNDCHARM [29, 30]. Final-state radiation (FSR) from charged final-state particles is incorporated using the PHOTOS package [31]. The total size of the inclusive MC samples is approximately 10 times that of the data.

The $D \to K_1(1270)e^+\nu_e$ decays are simulated with the ISGW2 model [2], and the $K_1(1270)$ is allowed to decay through all intermediate processes leading to the final state $K_S^0\pi\pi$. The $K_1(1270)$ resonance shape is parameterized by a relativistic Breit-Wigner function with a mass of $(1.253 \pm 0.007)\,\mathrm{GeV}/c^2$ and a width of $(90 \pm 20)\,\mathrm{MeV}$ [7]. Using the BFs of

$K_1(1270)$ measured by Belle [12] as input in the simulation gives good data/MC agreement in the kinematic distributions [11]. The $e^+e^- \to D\bar{D}$ signal MC samples, in which the D decays exclusively into signal modes while the $\bar{D}$ decays inclusively, are used to determine the detection efficiencies.

3 Measurement method and single-tag selection

At $\sqrt{s} = 3.773$ GeV, the $\psi(3770)$ resonance is produced in electron-positron annihilation, and then decays predominately into $D\bar{D}$ pairs without accompanying hadron(s), thereby offering a clean environment to investigate D decays with the double-tag (DT) method [32, 33]. In these cases, when a $\bar{D}$ meson is fully reconstructed, all of the remaining tracks and photons in the event must originate from the accompanying D meson. The fully reconstructed meson is called a single-tag (ST) $\bar{D}$. The ST $\bar{D}$ mesons are selected by reconstructing a $\bar{D}^0$ or D^- in one of the following decay modes: $K^+\pi^-$, $K^+\pi^-\pi^0$, $K^+\pi^-\pi^+\pi^-$, $K^+\pi^-\pi^+\pi^-\pi^0$ for neutral tags, and $K^+\pi^-\pi^-$, $K_S^0\pi^-$, $K^+\pi^-\pi^-\pi^0$, $K_S^0\pi^-\pi^0$, $K^+K^-\pi^-$ and $K_S^0\pi^+\pi^-\pi^-$ for charged tags. Using the ST $\bar{D}$ samples, the decays of $D \to K_S^0\pi\pi e^+\nu_e$ can be reliably identified from the recoiling tracks as DT events. The BF of the signal decay is then determined by

$$\mathcal{B}_{\mathrm{sig}} = \frac{N_{\mathrm{DT}}}{N_{\mathrm{ST}}^{\mathrm{tot}} \cdot \epsilon_{\mathrm{sig}}}, \tag{3.1}$$

where $N_{\mathrm{ST}}^{\mathrm{tot}}$ and N_{DT} are the ST and DT yields, $\epsilon_{\mathrm{sig}} = \sum_i \left[\left(\varepsilon_{\mathrm{DT}}^i N_{\mathrm{ST}}^i \right) / \left(\varepsilon_{\mathrm{ST}}^i N_{\mathrm{ST}}^{\mathrm{tot}} \right) \right]$ is the efficiency of detecting the SL decay in the presence of the ST $\bar{D}$ meson, reconstructed in any of the tag modes. Here, i denotes the tag mode, and ϵ_{ST} and ϵ_{DT} are the ST and DT efficiencies of selecting the ST and DT candidates, respectively. Using the BF of $K_1(1270) \to K_S^0\pi\pi$ given in the PDG [7], the BFs of the $D \to K_1(1270)e^+\nu_e$ decays can be obtained.

For the reconstruction and identification of K_S^0, $K^\pm$, $\pi^\pm$ and π^0, the same criteria are used as in refs. [34–39]. For any selected charged track, except for those used for reconstructing K_S^0 decays, the polar angle θ with respect to the z-axis (defined as the symmetry axis of the MDC) is required to satisfy $|\cos\theta| < 0.93$, and the point of closest approach to the interaction point (IP) must be within 1 cm in the plane perpendicular to the z axis and within ± 10 cm along the z axis. Particle identification (PID) for charged tracks combines measurements of the energy deposited in the MDC ($\mathrm{d}E/\mathrm{d}x$) and the flight time measured in the TOF to form likelihoods $\mathcal{L}(h)$ ($h = K, \pi$) for each hadron hypothesis h. Charged kaons and pions are identified by comparing the likelihoods for the kaon and pion hypotheses, $\mathcal{L}(K) > \mathcal{L}(\pi)$ and $\mathcal{L}(\pi) > \mathcal{L}(K)$, respectively.

The K_S^0 candidates are selected via the $K_S^0 \to \pi^+\pi^-$ decays, and hence they are reconstructed from pairs of oppositely charged tracks. For these two tracks, the distance of closest approach to the IP is required to be less than 20 cm along the z axis. The two charged tracks are constrained to originate from a common vertex that is required to be displaced from the IP by a flight distance of at least twice the vertex resolution. The invariant mass of the $\pi^+\pi^-$ pair is required to be within $(0.486, 0.510)$ GeV/c^2.

The π^0 candidates are reconstructed via $\pi^0 \to \gamma\gamma$ decays. Photon candidates are reconstructed from isolated electromagnetic showers detected in the EMC crystals. The deposited energy is required to be greater than 25 (50) MeV in the barrel (end-cap) region. To

Tag mode	ΔE (GeV)	$M_{\rm BC}$ (GeV/c^2)
$\bar{D}^0 \to K^+\pi^-$	$(-0.029, 0.027)$	$(1.858, 1.874)$
$\bar{D}^0 \to K^+\pi^-\pi^0$	$(-0.069, 0.038)$	$(1.858, 1.874)$
$\bar{D}^0 \to K^+\pi^-\pi^+\pi^-$	$(-0.031, 0.028)$	$(1.858, 1.874)$
$\bar{D}^0 \to K^+\pi^-\pi^+\pi^-\pi^0$	$(-0.040, 0.025)$	$(1.858, 1.874)$
$D^- \to K^+\pi^-\pi^-$	$(-0.025, 0.025)$	$(1.863, 1.877)$
$D^- \to K^+\pi^-\pi^-\pi^0$	$(-0.055, 0.040)$	$(1.863, 1.877)$
$D^- \to K^0_S\pi^-$	$(-0.025, 0.025)$	$(1.863, 1.877)$
$D^- \to K^0_S\pi^-\pi^0$	$(-0.055, 0.040)$	$(1.863, 1.877)$
$D^- \to K^0_S\pi^+\pi^-\pi^-$	$(-0.025, 0.025)$	$(1.863, 1.877)$
$D^- \to K^+K^-\pi^-$	$(-0.025, 0.025)$	$(1.863, 1.877)$

Table 1. Summary of the ΔE requirements and $M_{\rm BC}$ mass windows for the ten tag modes.

exclude showers that originate from charged tracks, the angle subtended by the EMC shower and the position of the closest charged track at the EMC must be greater than 10 degrees as measured from the IP. To further suppress fake photon candidates due to electronic noise or beam-related background, the measured EMC time is required to be within $[0, 700]$ ns from the event start time. The invariant mass of a photon pair is required to be within $(0.115, 0.150)$ GeV/c^2. To further improve the resolution of π^0 momentum $\vec{p}_{\pi^0}$, the invariant mass of the photon pair is constrained to the known π^0 mass [7] by applying a kinematic fit.

For the ST candidates $\bar{D}^0 \to K^+\pi^-$, the background contributions from cosmic rays and Bhabha events are rejected by using the analogue requirements as described in ref. [40]. First, the two charged tracks used must have a TOF time difference less than 5 ns and they must not be consistent with being a muon pair or an electron-positron pair. Second, there must be at least one EMC shower with an energy larger than 50 MeV or at least one additional charged track detected in the MDC.

The tagged $\bar{D}$ mesons are selected using two variables, the energy difference

$$\Delta E = E_{\bar{D}} - E_{\rm beam} \tag{3.2}$$

and the beam-constrained (BC) mass

$$M_{\rm BC} = \sqrt{E_{\rm beam}^2/c^4 - |\vec{p}_{\bar{D}}|^2/c^2}, \tag{3.3}$$

where $E_{\rm beam}$ is the beam energy, and $\vec{p}_{\bar{D}}$ and $E_{\bar{D}}$ are the momentum and the energy of the $\bar{D}$ candidate in the e^+e^- rest frame. For each tag mode, if there are multiple combinations in an event, only the one giving the minimum $|\Delta E|$ is retained for further analyses. Combinatorial background contributions are suppressed with a requirement on ΔE for each tag mode as described in refs. [10, 11]; the ΔE requirements are summarized in table 1.

To extract the yields of ST $\bar{D}$ mesons for each tag mode, binned maximum-likelihood fits are performed to the $M_{\rm BC}$ distributions of the accepted ST candidates. The signal
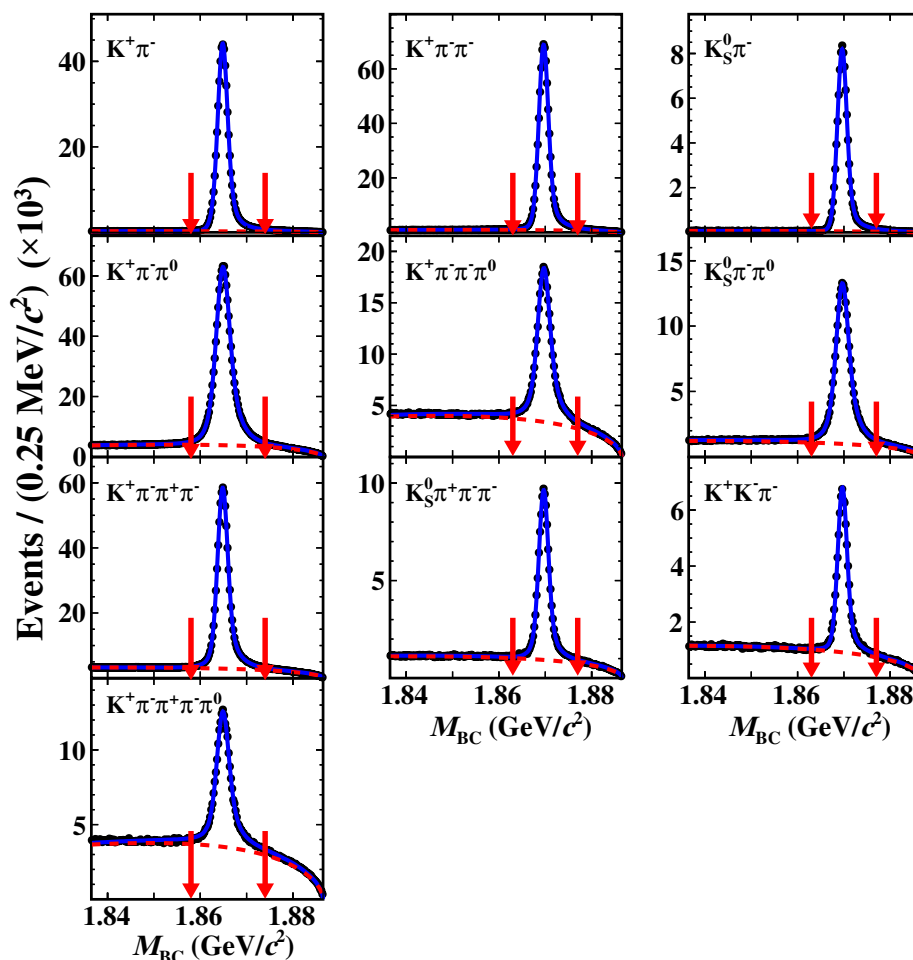
Figure 1. Fits to the M_{BC} distributions of the ST $\bar{D}$ candidates. The dots with error bars are the real data, the red dashed lines denote the background and the blue solid lines represent the overall fit. The arrows indicate the limits of the M_{BC} signal window.

is modeled by the MC-simulated shape convolved with a double-Gaussian function. The combinatorial background shape is described by an ARGUS function [41]. All parameters of the double-Gaussian function and the ARGUS function are left free in the fit. The numbers of ST $\bar{D}$ mesons are obtained by integrating over the $\bar{D}$ signal shape in the mass windows [10, 11] which are listed in table 1. The M_{BC} distributions of the accepted ST candidates in data for the ten tag modes are shown in figure 1. The ST yield and the ST efficiency ($\epsilon_{\mathrm{ST}}^{i}$) for each tag mode are summarized in table 2. The total ST yields of $\bar{D}^{0}$ and D^{-} candidates are $(250.5 \pm 0.4_{\mathrm{stat.}}) \times 10^{4}$ and $(153.2 \pm 0.3_{\mathrm{stat.}}) \times 10^{4}$, respectively.

4 Branching fractions

4.1 Selection of signal candidates

Candidates for the semileptonic decays $D \to K_{S}^{0}\pi\pi e^{+}\nu_{e}$ are reconstructed from the remaining tracks and showers that have not been used for the ST $\bar{D}$ reconstruction. The K_{S}^{0}, $\pi^{\pm}$

and π^0 candidates are selected with the same criteria as on the tag side. Positron PID uses the measured information in the MDC, TOF and EMC. Combined likelihoods ($\mathcal{L}'$) are calculated under the positron, pion, and kaon hypotheses. Positron candidates are required to satisfy $\mathcal{L}'(e) > 0.001$ and $\mathcal{L}'(e)/(\mathcal{L}'(e) + \mathcal{L}'(\pi) + \mathcal{L}'(K)) > 0.8$. To reduce background from hadrons, the positron candidate is further required to have a deposited energy in the EMC and momentum which satisfy $E/|\vec{p}|c > 0.18 \times \chi^2_{\mathrm{d}E/\mathrm{d}x} + 0.32$ [11], where E and $\vec{p}$ are the energy and momentum of positrons, $\chi^2_{\mathrm{d}E/\mathrm{d}x}$ is the difference between the measured energy loss and the expectation from the Bethe-Bloch curve normalized by the resolution for positrons. To partially compensate for the energy loss due to FSR and bremsstrahlung, the four momenta of neighboring photons with an energy greater than $50\,\mathrm{MeV}$ and within a cone of 5 degrees around the positron direction, are added back to the four-momenta of the positron candidates (FSR recovery).

When reconstructing the $D^0 \to K_S^0 \pi^- \pi^0 e^+ \nu_e$ decay, the π^0 mesons are required to have an energy greater than $0.22\,\mathrm{GeV}$ and a decay angle θ_{π^0} defined through $|\cos\theta_{\pi^0}| = |E_{\gamma_1} - E_{\gamma_2}|/|\vec{p}_{\pi^0}|c$, less than 0.83 to effectively veto fake π^0 candidates. Here, E_{γ_1} and E_{γ_2} are the energies of the two daughter photons of the π^0 candidate, and $\vec{p}_{\pi^0}$ is its reconstructed momentum. To suppress the background from $D^0 \to K_S^0 \pi^+ \pi^- \pi^0$ decays, $M_{K_S^0 \pi^- \pi^0 \pi^+_{e \to \pi}} < 1.78\,\mathrm{GeV}/c^2$ is required, where $\pi^+_{e \to \pi}$ is the positron candidate reconstructed under the pion mass hypothesis.

For the $D^+ \to K_S^0 \pi^+ \pi^- e^+ \nu_e$ decay, the positron must have the opposite charge to that of the tagged D^- meson and the two charged pions must have opposite charge. To suppress the background from $D^+ \to K_S^0 \pi^+ \pi^- \pi^+$ decays, the mass $M_{K_S^0 \pi^+ \pi^- \pi^+_{e \to \pi}}$ is required to be less than $1.83\,\mathrm{GeV}/c^2$. In order to reject background events from $D^+ \to K_S^0 \pi^+ \pi^0$ with the π^0 Dalitz decay $\pi^0 \to e^+ e^- \gamma$, the opening angle θ_α between e^+ and π^- is required to satisfy $\cos\theta_\alpha < 0.95$. To reject contamination from $D^+ \to K_S^0 \pi^+ \pi^- \pi^+ \pi^0$ decays, the mass $M_{K_S^0 \pi^+ \pi^- \pi^+_{e \to \pi} \pi^0}$ is required to satisfy $M_{K_S^0 \pi^+ \pi^- \pi^+_{e \to \pi} \pi^0} < 1.4\,\mathrm{GeV}/c^2$ when there is at least one π^0 candidate recoiling against the ST D^- meson in the event. Furthermore, the opening angle θ_β between the missing momentum (defined below) and the most energetic unused shower is required to satisfy $\cos\theta_\beta < 0.88$.

4.2 Measurement of branching fractions

To obtain information about the undetected neutrino, a kinematic quantity is defined as

$$M^2_{\mathrm{miss}} = E^2_{\mathrm{miss}}/c^4 - |\vec{p}_{\mathrm{miss}}|^2/c^2, \tag{4.1}$$

where E_{miss} and $\vec{p}_{\mathrm{miss}}$ are the total energy and momentum of all missing particles in the event, respectively. They are calculated using $E_{\mathrm{miss}} = E_{\mathrm{beam}} - \sum_i E_i$, $\vec{p}_{\mathrm{miss}} = -\vec{p}_D - \sum_i \vec{p}_i$ where E_i and $\vec{p}_i$ are the measured energy and momentum of particle i in the $e^+ e^-$ center-of-mass frame, and i runs over K_S^0, $\pi^\pm$, π^0 and e^+ of the signal candidate. In order to improve the M^2_{miss} resolution, a four-constraint (4-C) kinematic fit is employed. Here energy and momentum conservation is imposed, and the invariant masses of the D^0 and D^+ candidate particles are constrained to their known values. Then the momenta and energies from the kinematic fit are used to calculate M^2_{miss}.
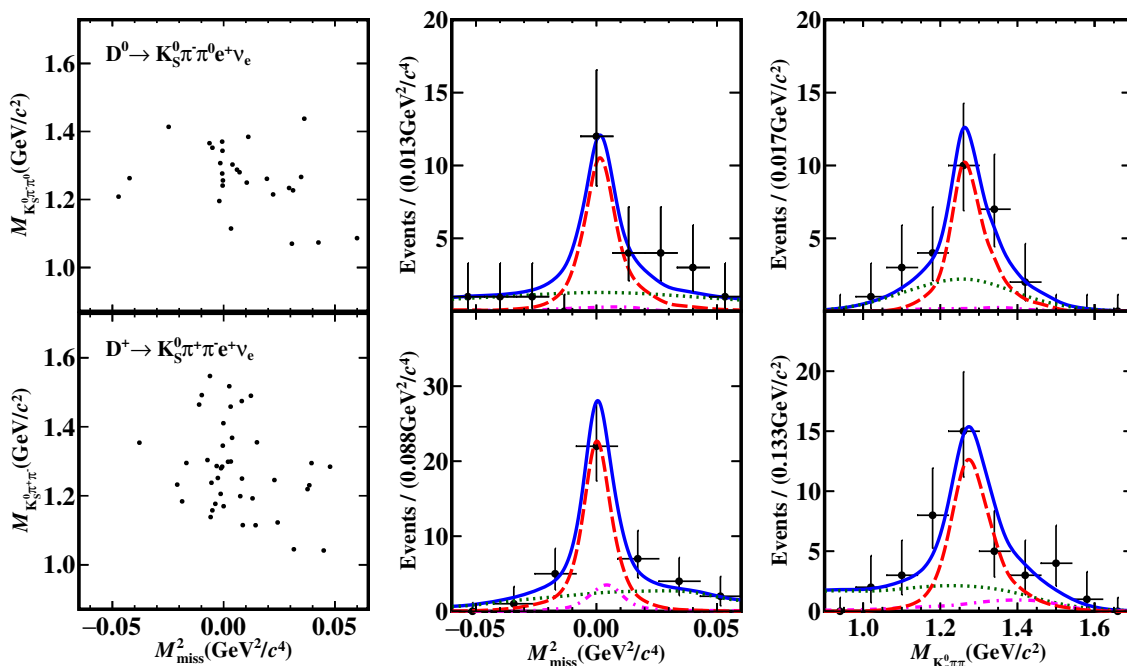
Figure 2. Distributions of M_{miss}^2 versus $M_{K_S^0\pi\pi}$ for the accepted semileptonic candidates (left column) and the projections on M_{miss}^2 (middle column) and $M_{K_S^0\pi\pi}$ (right column) of the two-dimensional fits. The top row is for $D^0 \to K_S^0\pi^-\pi^0 e^+\nu_e$ and the bottom row is for $D^+ \to K_S^0\pi^+\pi^- e^+\nu_e$. The dots with error bars are data. The blue solid line denotes the total fit. The red dashed line represents the signal. The green dotted and purple dash dotted lines represent the combinatorial background and peaking background of $D \to K_S^0\pi\pi$, respectively.

The distributions of M_{miss}^2 versus $M_{K_S^0\pi\pi}$ distributions of the candidate events for $D^0 \to K_S^0\pi^-\pi^0 e^+\nu_e$ and $D^+ \to K_S^0\pi^+\pi^- e^+\nu_e$ surviving in data are shown in figure 2 after combining all tag modes for D^0 or D^+. Signal events concentrate around zero in M_{miss}^2. They are found to cluster around the $K_1(1270)$ nominal mass in the $M_{K_S^0\pi\pi}$ distribution. The signal events are assumed to be from $D \to \bar{K}_1(1270)e^+\nu_e$ and potential contributions from non-resonant $K_S^0\pi\pi$ and $D \to \bar{K}_1(1400)e^+\nu_e$ will be discussed later. To determine the signal yield, a two-dimensional unbinned extended maximum-likelihood fit is performed on the M_{miss}^2 versus $M_{K_S^0\pi\pi}$ distributions of the accepted $D^0 \to K_S^0\pi^-\pi^0 e^+\nu_e$ and $D^+ \to K_S^0\pi^+\pi^- e^+\nu_e$ candidate events, respectively. The two-dimensional signal and background shapes are derived from the signal and inclusive MC samples, respectively. The numbers of peaking background events are fixed based on the estimation from the simulated samples, while the yields of signal and combinatorial background are free parameters. The two-dimensional probability density functions of signal and background are modeled by using RooNDKeysPdf [42].

The one-dimensional fit projections to the M_{miss}^2 and $M_{K_S^0\pi\pi}$ distributions of $D^0 \to K_S^0\pi^-\pi^0 e^+\nu_e$ and $D^+ \to K_S^0\pi^+\pi^- e^+\nu_e$ are shown in figure 2. The fits return event yields of $16.5^{+5.1}_{-4.5}$ for the $D^0 \to K_1(1270)^- e^+\nu_e$ signal and $20.2^{+6.2}_{-5.4}$ for the $D^+ \to \bar{K}_1(1270)^0 e^+\nu_e$ signal. The DT yields and signal efficiencies are summarized in table 2. The uncertainties in table 2 are only statistical, and the systematic uncertainties will be discussed in section 5. The statistical significance of the signal is estimated to be 5.4σ for $D^0 \to K_1(1270)^- e^+\nu_e$ and

Tag mode	N_{ST}^i ($\times 10^3$)	ϵ_{ST}^i (%)	ϵ_{sig}^i (%)	$\bar{\epsilon}_{\text{sig}}$ (%)	N_{DT}
$\bar{D}^0 \to K^+\pi^-$	540.7±0.8	66.57 ± 0.09	4.86±0.05		
$\bar{D}^0 \to K^+\pi^-\pi^0$	1066.8±1.2	34.76 ± 0.04	4.10±0.03	3.89±0.03	$16.5^{+5.1}_{-4.5}$
$\bar{D}^0 \to K^+\pi^-\pi^+\pi^-$	736.3±1.2	41.22 ± 0.05	3.30±0.04		
$\bar{D}^0 \to K^+\pi^-\pi^+\pi^-\pi^0$	162.0±0.4	15.94 ± 0.05	2.02±0.04		
$D^- \to K^+\pi^-\pi^-$	800.6±1.0	51.10 ± 0.06	9.99±0.11		
$D^- \to K^+\pi^-\pi^-\pi^0$	253.0±0.6	24.54 ± 0.06	7.83±0.17		
$D^- \to K_S^0\pi^-$	93.3±0.3	50.90 ± 0.17	9.99±0.33	8.96±0.09	$20.2^{+6.2}_{-5.4}$
$D^- \to K_S^0\pi^-\pi^0$	208.9±0.5	25.15 ± 0.06	7.88±0.21		
$D^- \to K_S^0\pi^-\pi^-\pi^+$	107.5±0.4	29.47 ± 0.09	5.23±0.22		
$D^- \to K^+K^-\pi^-$	68.9±0.3	41.23 ± 0.18	9.00±0.35		

Table 2. Summary of ST yields N_{ST}^i, ST efficiencies ϵ_{ST}^i (%), signal efficiencies ϵ_{sig}^i of different tag modes i, where the uncertainties are statistical. The last two columns are the weighted efficiencies $\bar{\epsilon}_{\text{sig}}$ and signal yields N_{DT}.

5.6σ for $D^+ \to K_1(1270)^0 e^+\nu_e$, by comparing the likelihoods with and without the signal component, and taking the change in the number of degrees of freedom into account. The significances of $D^0 \to K_S^0\pi^-\pi^0 e^+\nu_e$ and $D^+ \to K_S^0\pi^+\pi^- e^+\nu_e$ are 4.5σ and 4.0σ, respectively, after accounting for systematic uncertainties associated with the 2D fits.

Inserting N_{DT}, $\bar{\epsilon}_{\text{sig}}$, and $N_{\text{ST}}^{\text{tot}}$ into eq. (3.1) yields the BF for each decay. Using the world average BFs of $\mathcal{B}(K_1(1270)^- \to K_S^0\pi^-\pi^0) = (16.00\pm3.45)\%$ and $\mathcal{B}(\bar{K}_1(1270)^0 \to K_S^0\pi^+\pi^-) = (11.67 \pm 2.26)\%$,[1] the absolute BFs of $D^0 \to K_1(1270)^- e^+\nu_e$ and $D^+ \to \bar{K}_1(1270)^0 e^+\nu_e$ are also determined. The obtained BFs $\mathcal{B}_{\text{sig}}$ are summarized in table 3 and are in agreement with those obtained from measurements with a charged kaon in the final state [10, 11]. Therefore the two sets of the results are combined to yield the values $\mathcal{B}_{\text{com}}$, which are also given in table 3.

In addition to the $D \to \bar{K}_1(1270)e^+\nu_e$ contribution to the $D \to K_S^0\pi\pi e^+\nu_e$ signal, the one from non-resonant $K_S^0\pi\pi$ events could be sizeable. However, the latter component cannot be accurately determined due to the lack of knowledge regarding its fraction and limited statistics. To evaluate its effect on the nominal fit, a 10% contribution relative to the $K_1(1270)$ component from non-resonant $K_S^0\pi\pi$ is imposed in the fit. The shape of

---

[1] $\mathcal{B}_{K_1^0 \to K_S^0\pi^+\pi^-} = \mathcal{B}_{K_1^0 \to K^0\pi^+\pi^-} \times \frac{1}{2} \times \mathcal{B}_{K_S^0 \to \pi^+\pi^-}$

$= \frac{\mathcal{B}_{K_S^0 \to \pi^+\pi^-}}{2} \times \left(\frac{1}{3} \times \mathcal{B}_{K_1 \to K\rho} + \frac{4}{9} \times \mathcal{B}_{K_1 \to K^*(892)\pi} + \frac{4}{9} \times \mathcal{B}_{K_1 \to K_0^*(1430)\pi} \times \mathcal{B}_{K_0^*(1430) \to K\pi} \right.$

$\left. + \mathcal{B}_{K_1 \to K+\omega} \times \mathcal{B}_{\omega \to \pi^+\pi^-} \right),$

$\mathcal{B}_{K_1^- \to K_S^0\pi^-\pi^0} = \mathcal{B}_{K_1^- \to K^0\pi^-\pi^0} \times \frac{1}{2} \times \mathcal{B}_{K_S^0 \to \pi^+\pi^-}$

$= \frac{\mathcal{B}_{K_S^0 \to \pi^+\pi^-}}{2} \times \left(\frac{2}{3} \times \mathcal{B}_{K_1 \to K\rho} + \frac{4}{9} \times \mathcal{B}_{K_1 \to K^*(892)\pi} + \frac{4}{9} \times \mathcal{B}_{K_1 \to K_0^*(1430)\pi} \times \mathcal{B}_{K_0^*(1430) \to K\pi} \right),$

where K_1 denotes $K_1(1270)$ and K_S^0 is reconstructed via $K_S^0 \to \pi^+\pi^-$.

Decay mode	$\mathcal{B}_{\rm sig}$ $(\times 10^{-4})$	$\mathcal{B}_{\rm com}$ $(\times 10^{-4})$
$D^0 \to K_S^0 \pi^- \pi^0 e^+ \nu_e$	$(1.69^{+0.53}_{-0.46} \pm 0.15)$	/
$D^+ \to K_S^0 \pi^+ \pi^- e^+ \nu_e$	$(1.47^{+0.45}_{-0.40} \pm 0.14)$	/
$D^0 \to K_1(1270)^- e^+ \nu_e$	$(10.6^{+3.3}_{-2.8} \pm 0.9 \pm 2.3)$	$(10.8^{+1.4+0.8}_{-1.3-1.0} \pm 2.1)$
$D^+ \to \bar{K}_1(1270)^0 e^+ \nu_e$	$(12.9^{+4.0}_{-3.5} \pm 1.0 \pm 2.5)$	$(17.0^{+2.6}_{-2.3} \pm 1.3 \pm 3.5)$

Table 3. Summary of measured BFs $\mathcal{B}_{\rm sig}$ for different decays and combined BFs $\mathcal{B}_{\rm com}$ for $D \to K_1(1270)e^+\nu_e$ decays. The first and second uncertainties are statistical and systematic, respectively. For $D \to K_1(1270)e^+\nu_e$ modes, the third uncertainty originates from the assumed BFs of $K_1(1270)$ decays [7].

		$\mathcal{B}(D \to K_S^0 \pi\pi e^+ \nu_e) \times 10^{-4}$	$\mathcal{B}(D \to \bar{K}_1(1270)e^+ \nu_e) \times 10^{-4}$
D^0	I	$1.69^{+0.53}_{-0.46}$	$10.6^{+3.3}_{-2.9}$
	II	$1.68^{+0.52}_{-0.45}$	$9.6^{+3.0}_{-2.6}$
	III	$1.64^{+0.53}_{-0.45}$	$9.4^{+3.0}_{-2.6}$
D^+	I	$1.47^{+0.45}_{-0.40}$	$12.6^{+3.9}_{-3.5}$
	II	$1.60^{+0.46}_{-0.41}$	$12.5^{+3.5}_{-3.2}$
	III	$1.56^{+0.42}_{-0.41}$	$12.2^{+3.3}_{-3.2}$

Table 4. Summary of BFs obtained from the nominal fits (I), the fits with the inclusion of the non-resonant contribution (II), and the fits with the inclusion of the $K_1(1400)$ contribution (III). All the quoted uncertainties are statistical only.

the non-resonant component is modeled using simulated $D \to K_S^0 \pi\pi e^+ \nu_e$ events generated evenly in the available phase space. The yields of non-resonant and $K_1(1270)$ contributions are combined and treated as signal events to evaluate $\mathcal{B}(D \to K_S^0 \pi\pi e^+ \nu_e)$. The yields of $D \to \bar{K}_1(1270)e^+ \nu_e$ are used to evaluate $\mathcal{B}(D^+ \to K_1(1270)^- e^+ \nu_e)$. The obtained BFs with the 10% non-resonant contribution are summarized in table 4, specifically in row II.

Furthermore, there is a possible contribution from $D \to \bar{K}_1(1400)e^+ \nu_e$ decay. It is also challenging to determine the fraction due to the large intrinsic width of $K_1(1400)$. A 10% contribution relative to $D \to \bar{K}_1(1270)e^+ \nu_e$ from $D \to \bar{K}_1(1400)e^+ \nu_e$ decays is considered to evaluate its effect on the nominal fit result. The $D \to \bar{K}_1(1400)(\to K_S^0 \pi\pi)e^+ \nu_e$ decays are simulated with the ISGW2 model, and the $K_1(1400)$ resonance shape is parameterized by a relativistic Breit-Wigner function with the mass and width fixed to the PDG values [7]. The yields of $K_1(1400)$ and $K_1(1270)$ are combined and treated as signal events to evaluate $\mathcal{B}(D \to K_S^0 \pi\pi e^+ \nu_e)$. The yields of $D \to \bar{K}_1(1270)e^+ \nu_e$ are used to evaluate $\mathcal{B}(D^+ \to K_1(1270)^- e^+ \nu_e)$. The obtained BFs with the 10% $K_1(1400)$ contribution are summarized in table 4, specifically in row III.

5 Systematic uncertainties

While in the BF determination using eq. (3.1) the uncertainties associated with the ST candidate selection cancel, the following sources of systematic uncertainties must be considered.

- The uncertainty in the total yield of ST $\bar{D}$ mesons is assigned to be 0.5% [10, 11].

- $\pi^{\pm}$ tracking and PID efficiencies. The data/MC differences of $\pi^{\pm}$ tracking and PID efficiencies are re-weighted by the corresponding $\pi^{\pm}$ momentum spectra of signal MC events. The systematic uncertainty of tracking (PID) efficiency is assigned to be 0.2% (0.3%) per $\pi^{\pm}$, based on the residual statistical uncertainties of the measured data/MC differences.

- $e^{\pm}$ tracking and PID efficiencies. The systematic uncertainties originating from e^{+} tracking and PID efficiencies are studied by using a control sample of $e^{+}e^{-} \to \gamma e^{+}e^{-}$ events. The tracking and PID efficiencies of MC are also re-weighted in momentum and $\cos\theta$ to match the $D \to K_S^0 \pi\pi e^{+}\nu_e$ data. The systematic uncertainty of tracking (PID) efficiency is assigned to be 0.3%(0.3%) per $e^{\pm}$.

- K_S^0 reconstruction. The systematic uncertainty associated with K_S^0 reconstruction is studied with control samples of the decays $J/\psi \to K^{*\pm}K^{\mp}$ and $J/\psi \to \phi K_S^0 K^{\pm}\pi^{\mp}$ [43]. The systematic uncertainty for each K_S^0 is assigned as 1.5%.

- π^0 reconstruction. The systematic uncertainty of π^0 reconstruction is assigned as 2.0% per π^0 from studies of the DT $D^0\bar{D}^0$ hadronic decay samples [34].

- Two-dimensional fit. To estimate the uncertainty arising from the signal shape used in the fit, the mass and width of $K_1(1270)$ are varied by $\pm1\sigma$. To take into account the potential resolution difference between data and MC simulation in the fit, a convolution of a Gaussian function is considered for M_{miss}^2 and $M_{K_S^0\pi\pi}$. The peaking background yields are varied by 20.0% after considering their statistical fluctuations. The uncertainties of combinatorial background shapes are estimated by varying the smoothing parameters [42]. The associated systematic uncertainties are summarized in table 5.

- Signal generator. To estimate the systematic uncertainty associated with the signal generator, alternative signal MC events are generated using a phase-space model. The changes in the measured BFs using this alternative MC simulation are 6.5% for $\mathcal{B}(D^0 \to K_S^0\pi^-\pi^0 e^+\nu_e)$ and 4.0% for $\mathcal{B}(D^+ \to K_S^0\pi^+\pi^- e^+\nu_e)$.

- $K_1(1270)$ subdecays. The uncertainties in the ratios of $K_1(1270)$ subdecays are assigned by remeasuring the BFs based on PDG models [7]. A systematic uncertainty of 2.0% is assigned both for $\mathcal{B}(D^0 \to K_S^0\pi^-\pi^0 e^+\nu_e)$ and $\mathcal{B}(D^+ \to K_S^0\pi^+\pi^- e^+\nu_e)$.

- MC sample size. The systematic uncertainty due to the limited size of the MC sample is assigned to be 1.0% by $\sqrt{\sum_i \left(f_i \frac{\sigma_{\epsilon_i}}{\epsilon_i}\right)^2}$, where f_i is the tag yield fraction, and ϵ_i and σ_{ϵ_i} are signal efficiency and the corresponding uncertainty of tag mode i, respectively.

- FSR recovery. The uncertainty from FSR recovery is assigned to be 0.3% following ref. [44].

Uncertainty (%)	$K_S^0\pi^-\pi^0 e^+\nu_e$	$K_S^0\pi^+\pi^- e^+\nu_e$
Signal shape	3.0	5.0
Resolution	2.4	3.3
Peaking background	1.3	2.1
Combinatorial background	1.0	3.8
Total	4.3	7.4

Table 5. Systematic uncertainties from the 2D fits.

Uncertainty (%)	$K_S^0\pi^-\pi^0 e^+\nu_e$	$K_S^0\pi^+\pi^- e^+\nu_e$
$N_{\rm ST}$	0.5	0.5
$\pi^\pm, e^\pm$ tracking	0.5	0.7
$\pi^\pm, e^\pm$ PID	0.6	0.9
K_S^0 reconstruction	1.5	1.5
π^0 reconstruction	2.0	/
Two-dimensional simultaneous fit	4.2	7.4
Signal generator	6.5	4.0
$K_1(1270)$ subdecays	2.0	2.0
MC sample size	1.0	1.0
FSR recovery	0.3	0.3
Total	8.6	9.0

Table 6. Relative systematic uncertainties in the BF measurements. The systematical uncertainties are evaluated under the assumption that all signal events are from the $D \to \bar{K}_1(1270)e^+\nu_e$ decays. The uncertainties related to the possible non-resonant and $K_1(1400)$ contributions are not considered.

The systematical uncertainties are evaluated by assuming all signal events are from the $D \to \bar{K}_1(1270)e^+\nu_e$ decays. As summarized in table 4, in the presence of the 10% non-resonant component, the BFs values of $\mathcal{B}(D^0 \to K_1(1270)^- e^+\nu_e)$ and $\mathcal{B}(D^+ \to \bar{K}_1(1270)^0 e^+\nu_e)$ are reduced by 9% and 1%, respectively. In the same way, if the 10% $K_1(1400)$ component is considered, $\mathcal{B}(D^0 \to K_1(1270)^- e^+\nu_e)$ and $\mathcal{B}(D^+ \to \bar{K}_1(1270)^0 e^+\nu_e)$ will be reduced by 10% and 3%, respectively.

The total systematic uncertainty is estimated by adding all the individual contributions in quadrature. The sources of the systematic uncertainties in the BF measurements are summarized in table 6. They are assigned relatively to the measured BFs.

6 Summary

By analyzing a data sample corresponding to an integrated luminosity of $2.93\,\mathrm{fb}^{-1}$ collected at $\sqrt{s} = 3.773\,\mathrm{GeV}$ with the BESIII detector, the first observations of the semileptonic decays $D^0 \to K_S^0\pi^-\pi^0 e^+\nu_e$ and $D^+ \to K_S^0\pi^+\pi^- e^+\nu_e$ are obtained with statistical significances of 5.4σ and 5.6σ, respectively. Under the assumption that $K_1(1270)$ is the only contributing

source, the resulting BFs are summarized in table 3. The measured BFs of $D \to \bar{K}_1(1270)e^+\nu_e$ decays are consistent with previous measurements using $\bar{K}_1(1270) \to K^-\pi^+\pi^{(-,0)}$ [10, 11]. The combined BFs of $D \to \bar{K}_1(1270)e^+\nu_e$ agree with the CLFQM and LCSR predictions when $\theta_{K_1} \approx 33°$ or $57°$ [4, 5] and contradict the predictions reported in ref. [6] when setting the value of θ_{K_1} negative.

With approximately six times more data coming from BESIII at $\sqrt{s} = 3.773\,\text{GeV}$ in the foreseen future [22, 45], a thorough investigation with the enlarged data samples in the four K_1 channels $(K^-\pi^+\pi^+, K_S^0\pi^0\pi^+, K_S^0\pi^+\pi^-, K^-\pi^+\pi^0)$ will be possible to further elucidate the knowledge on $K_1(1270)$ and $K_1(1400)$ meson in a systematic fashion.

Acknowledgments

References

[1] N. Isgur, D. Scora, B. Grinstein and M.B. Wise, *Semileptonic B and D Decays in the Quark Model*, *Phys. Rev. D* **39** (1989) 799 [INSPIRE].

[2] D. Scora and N. Isgur, *Semileptonic meson decays in the quark model: An update*, *Phys. Rev. D* **52** (1995) 2783 [hep-ph/9503486] [INSPIRE].

[3] H. Hatanaka and K.C. Yang, $K_1(1270)$–$K_1(1400)$ *Mixing angle and new-physics effects in* $B \to K_1 \ell^+ \ell^-$ *decays*, *Phys. Rev. D* **78** (2008) 074007 [arXiv:0808.3731] [INSPIRE].

[4] H.Y. Cheng and X.W. Kang, *Branching fractions of semileptonic D and D_s decays from the covariant light-front quark model*, *Eur. Phys. J. C* **77** (2017) 587 [*Erratum ibid.* **77** (2017) 863] [arXiv:1707.02851] [INSPIRE].

[5] S. Momeni, *Helicity form factors for $D_{(s)} \to A\ell\nu$ process in the light-cone QCD sum rules approach*, *Eur. Phys. J. C* **80** (2020) 553 [arXiv:2004.02522] [INSPIRE].

[6] S. Momeni and R. Khosravi, *Semileptonic $D_{(s)} \to A\ell^+\nu$ and nonleptonic $D \to K_1(1270, 1400)\pi$ decays in LCSR*, *J. Phys. G* **46** (2019) 105006 [arXiv:1903.00860] [INSPIRE].

[7] PARTICLE DATA collaboration, *Review of Particle Physics*, *Prog. Theor. Exp. Phys.* **2022** (2022) 083C01 [INSPIRE].

[8] W. Wang, F.S. Yu and Z.X. Zhao, *Novel Method to Reliably Determine the Photon Helicity in* $B \to K_1\gamma$, *Phys. Rev. Lett.* **125** (2020) 051802 [arXiv:1909.13083] [INSPIRE].

[9] L. Bian, L. Sun and W. Wang, *Up-down asymmetries and angular distributions in $D \to K_1 \ell^+ \nu_\ell$*, *Phys. Rev. D* **104** (2021) 053003 [arXiv:2105.06207] [INSPIRE].

[10] BESIII collaboration, *Observation of the Semileptonic D^+ Decay into the $\bar{K}_1(1270)^0$ Axial-Vector Meson*, *Phys. Rev. Lett.* **123** (2019) 231801 [arXiv:1907.11370] [INSPIRE].

[11] BESIII collaboration, *Observation of $D^0 \to K_1(1270)^- e^+ \nu_e$*, *Phys. Rev. Lett.* **127** (2021) 131801 [arXiv:2102.10850] [INSPIRE].

[12] BELLE collaboration, *Study of the $K^+\pi^+\pi^-$ final state in $B^+ \to J/\psi K^+\pi^+\pi^-$ and $B^+ \to \psi' K^+\pi^+\pi^-$*, *Phys. Rev. D* **83** (2011) 032005 [arXiv:1009.5256] [INSPIRE].

[13] BESIII collaboration, *Amplitude analysis and branching fraction measurement of $D_s^+ \to K^- K^+ \pi^+ \pi^0$*, *Phys. Rev. D* **104** (2021) 032011 [arXiv:2103.02482] [INSPIRE].

[14] CLEO collaboration, *Amplitude analysis of $D^0 \to K^+ K^- \pi^+ \pi^-$*, *Phys. Rev. D* **85** (2012) 122002 [arXiv:1201.5716] [INSPIRE].

[15] BESIII collaboration, *Amplitude analysis of $D^0 \to K^- \pi^+ \pi^+ \pi^-$*, *Phys. Rev. D* **95** (2017) 072010 [arXiv:1701.08591] [INSPIRE].

[16] LHCb collaboration, *Studies of the resonance structure in $D^0 \to K^\mp \pi^\pm \pi^\pm \pi^\mp$ decays*, *Eur. Phys. J. C* **78** (2018) 443 [arXiv:1712.08609] [INSPIRE].

[17] P. d'Argent et al., *Amplitude Analyses of $D^0 \to \pi^+\pi^-\pi^+\pi^-$ and $D^0 \to K^+K^-\pi^+\pi^-$ Decays*, *JHEP* **05** (2017) 143 [arXiv:1703.08505] [INSPIRE].

[18] P.F. Guo, D. Wang and F.S. Yu, *Strange Axial-vector Mesons in D Meson Decays*, *Nucl. Phys. Rev.* **36** (2019) 125 [arXiv:1801.09582] [INSPIRE].

[19] BESIII collaboration, *Measurement of the integrated luminosities of the data taken by BESIII at $\sqrt{s} = 3.650$ and 3.773 GeV*, *Chin. Phys. C* **37** (2013) 123001 [arXiv:1307.2022] [INSPIRE].

[20] BESIII collaboration, *Design and Construction of the BESIII Detector*, *Nucl. Instrum. Meth. A* **614** (2010) 345 [arXiv:0911.4960] [INSPIRE].

[21] C.H. Yu, Y. Zhang, Q. Qin, J.Q. Wang and G. Xu et al., *BEPCII Performance and Beam Dynamics Studies on Luminosity*, in the proceedings of the *7th International Particle Accelerator Conference (IPAC 2016)*, Busan, South Korea, 8–13 May 2016 [DOI:10.18429/JACoW-IPAC2016-TUYA01] [INSPIRE].

[22] BESIII collaboration, *Future Physics Programme of BESIII*, *Chin. Phys. C* **44** (2020) 040001 [arXiv:1912.05983] [INSPIRE].

[23] GEANT4 collaboration, *GEANT4 — a simulation toolkit*, *Nucl. Instrum. Meth. A* **506** (2003) 250 [INSPIRE].

[24] K.X. Huang et al., *Method for detector description transformation to Unity and application in BESIII*, *Nucl. Sci. Tech.* **33** (2022) 142 [`arXiv:2206.10117`] [INSPIRE].

[25] S. Jadach, B.F.L. Ward and Z. Was, *Coherent exclusive exponentiation for precision Monte Carlo calculations*, *Phys. Rev. D* **63** (2001) 113009 [`hep-ph/0006359`] [INSPIRE].

[26] S. Jadach, B.F.L. Ward and Z. Was, *The precision Monte Carlo event generator KK for two fermion final states in e^+e^- collisions*, *Comput. Phys. Commun.* **130** (2000) 260 [`hep-ph/9912214`] [INSPIRE].

[27] R.G. Ping, *Event generators at BESIII*, *Chin. Phys. C* **32** (2008) 599 [INSPIRE].

[28] D.J. Lange, *The EvtGen particle decay simulation package*, *Nucl. Instrum. Meth. A* **462** (2001) 152 [INSPIRE].

[29] J.C. Chen, G.S. Huang, X.R. Qi, D.H. Zhang and Y.S. Zhu, *Event generator for J/ψ and $\psi(2S)$ decay*, *Phys. Rev. D* **62** (2000) 034003 [INSPIRE].

[30] R.L. Yang, R.G. Ping and H. Chen, *Tuning and Validation of the Lundcharm Model with J/ψ Decays*, *Chin. Phys. Lett.* **31** (2014) 061301 [INSPIRE].

[31] E. Richter-Was, *QED bremsstrahlung in semileptonic B and leptonic tau decays*, *Phys. Lett. B* **303** (1993) 163 [INSPIRE].

[32] MARK-III collaboration, *Direct Measurements of Charmed d Meson Hadronic Branching Fractions*, *Phys. Rev. Lett.* **56** (1986) 2140 [INSPIRE].

[33] H.B. Li and X.R. Lyu, *Study of the standard model with weak decays of charmed hadrons at BESIII*, *Natl. Sci. Rev.* **8** (2021) nwab181 [`arXiv:2103.00908`] [INSPIRE].

[34] BESIII collaboration, *Improved measurement of the absolute branching fraction of $D^+ \to \bar{K}^0 \mu^+ \nu_\mu$*, *Eur. Phys. J. C* **76** (2016) 369 [`arXiv:1605.00068`] [INSPIRE].

[35] BESIII collaboration, *Measurement of the absolute branching fraction of $D^+ \to \bar{K}^0 e^+ \nu_e$ via $\bar{K}^0 \to \pi^0 \pi^0$*, *Chin. Phys. C* **40** (2016) 113001 [`arXiv:1605.00208`] [INSPIRE].

[36] BESIII collaboration, *Measurement of the branching fraction for the semi-leptonic decay $D^{0(+)} \to \pi^{-(0)} \mu^+ \nu_\mu$ and test of lepton universality*, *Phys. Rev. Lett.* **121** (2018) 171803 [`arXiv:1802.05492`] [INSPIRE].

[37] BESIII collaboration, *Observation of the Semileptonic Decay $D^0 \to a_0(980)^- e^+ \nu_e$ and Evidence for $D^+ \to a_0(980)^0 e^+ \nu_e$*, *Phys. Rev. Lett.* **121** (2018) 081802 [`arXiv:1803.02166`] [INSPIRE].

[38] BESIII collaboration, *Study of the $D^0 \to K^- \mu^+ \nu_\mu$ dynamics and test of lepton flavor universality with $D^0 \to K^- \ell^+ \nu_\ell$ decays*, *Phys. Rev. Lett.* **122** (2019) 011804 [`arXiv:1810.03127`] [INSPIRE].

[39] BESIII collaboration, *Observation of $D^+ \to f_0(500) e^+ \nu_e$ and Improved Measurements of $D \to \rho e^+ \nu_e$*, *Phys. Rev. Lett.* **122** (2019) 062001 [`arXiv:1809.06496`] [INSPIRE].

[40] BESIII collaboration, *Measurement of the $D \to K^- \pi^+$ strong phase difference in $\psi(3770) \to D^0 \overline{D}^0$*, *Phys. Lett. B* **734** (2014) 227 [`arXiv:1404.4691`] [INSPIRE].

[41] ARGUS collaboration, *Search for Hadronic $b \to u$ Decays*, *Phys. Lett. B* **241** (1990) 278 [INSPIRE].

[42] W. Verkerke and D.P. Kirkby, *The RooFit toolkit for data modeling*, *eConf C* **0303241** (2003) MOLT007 [`physics/0306116`] [INSPIRE].

[43] BESIII collaboration, *Study of the decay $D^0 \to \bar{K}^0 \pi^- e^+ \nu_e$*, *Phys. Rev. D* **99** (2019) 011103 [`arXiv:1811.11349`] [INSPIRE].

[44] BESIII collaboration, *Study of Dynamics of $D^0 \to K^- e^+ \nu_e$ and $D^0 \to \pi^- e^+ \nu_e$ Decays*, *Phys. Rev. D* **92** (2015) 072012 [`arXiv:1508.07560`] [INSPIRE].

[45] B.C. Ke, J. Koponen, H.B. Li and Y. Zheng, *Recent Progress in Leptonic and Semileptonic Decays of Charmed Hadrons*, *Annu. Rev. Nucl. Part. Sci.* **73** (2023) 285 [`arXiv:2310.05228`] [INSPIRE].

The BESIII collaboration

M. Ablikim[1], M.N. Achasov[5,b], P. Adlarson[75], X.C. Ai[81], R. Aliberti[36], A. Amoroso[74A,74C], M.R. An[40], Q. An[71,58], Y. Bai[57], O. Bakina[37], I. Balossino[30A], Y. Ban[47,g], V. Batozskaya[1,45], K. Begzsuren[33], N. Berger[36], M. Berlowski[45], M. Bertani[29A], D. Bettoni[30A], F. Bianchi[74A,74C], E. Bianco[74A,74C], A. Bortone[74A,74C], I. Boyko[37], R.A. Briere[6], A. Brueggemann[68], H. Cai[76], X. Cai[1,58], A. Calcaterra[29A], G.F. Cao[1,63], N. Cao[1,63], S.A. Cetin[62A], J.F. Chang[1,58], T.T. Chang[77], W.L. Chang[1,63], G.R. Che[44], G. Chelkov[37,a], C. Chen[44], Chao Chen[55], G. Chen[1], H.S. Chen[1,63], M.L. Chen[1,58,63], S.J. Chen[43], S.M. Chen[61], T. Chen[1,63], X.R. Chen[32,63], X.T. Chen[1,63], Y.B. Chen[1,58], Y.Q. Chen[35], Z.J. Chen[26,h], W.S. Cheng[74C], S.K. Choi[11], X. Chu[44], G. Cibinetto[30A], S.C. Coen[4], F. Cossio[74C], J.J. Cui[50], H.L. Dai[1,58], J.P. Dai[79], A. Dbeyssi[19], R.E. de Boer[4], D. Dedovich[37], Z.Y. Deng[1], A. Denig[36], I. Denysenko[37], M. Destefanis[74A,74C], F. De Mori[74A,74C], B. Ding[66,1], X.X. Ding[47,g], Y. Ding[41], Y. Ding[35], J. Dong[1,58], L.Y. Dong[1,63], M.Y. Dong[1,58,63], X. Dong[76], M.C. Du[1], S.X. Du[81], Z.H. Duan[43], P. Egorov[37,a], Y.L. Fan[76], J. Fang[1,58], S.S. Fang[1,63], W.X. Fang[1], Y. Fang[1], R. Farinelli[30A], L. Fava[74B,74C], F. Feldbauer[4], G. Felici[29A], C.Q. Feng[71,58], J.H. Feng[59], K. Fischer[69], M. Fritsch[4], C. Fritzsch[68], C.D. Fu[1], J.L. Fu[63], Y.W. Fu[1], H. Gao[63], Y.N. Gao[47,g], Yang Gao[71,58], S. Garbolino[74C], I. Garzia[30A,30B], P.T. Ge[76], Z.W. Ge[43], C. Geng[59], E.M. Gersabeck[67], A. Gilman[69], K. Goetzen[14], L. Gong[41], W.X. Gong[1,58], W. Gradl[36], S. Gramigna[30A,30B], M. Greco[74A,74C], M.H. Gu[1,58], Y.T. Gu[16], C.Y. Guan[1,63], Z.L. Guan[23], A.Q. Guo[32,63], L.B. Guo[42], M.J. Guo[50], R.P. Guo[49], Y.P. Guo[13,f], A. Guskov[37,a], T.T. Han[50], W.Y. Han[40], X.Q. Hao[20], F.A. Harris[65], K.K. He[55], K.L. He[1,63], F.H.H. Heinsius[4], C.H. Heinz[36], Y.K. Heng[1,58,63], C. Herold[60], T. Holtmann[4], P.C. Hong[13,f], G.Y. Hou[1,63], X.T. Hou[1,63], Y.R. Hou[63], Z.L. Hou[1], H.M. Hu[1,63], J.F. Hu[56,i], T. Hu[1,58,63], Y. Hu[1], G.S. Huang[71,58], K.X. Huang[59], L.Q. Huang[32,63], X.T. Huang[50], Y.P. Huang[1], T. Hussain[73], N. Hüsken[28,36], W. Imoehl[28], J. Jackson[28], S. Jaeger[4], S. Janchiv[33], J.H. Jeong[11], Q. Ji[1], Q.P. Ji[20], X.B. Ji[1,63], X.L. Ji[1,58], Y.Y. Ji[50], X.Q. Jia[50], Z.K. Jia[71,58], H.J. Jiang[76], P.C. Jiang[47,g], S.S. Jiang[40], T.J. Jiang[17], X.S. Jiang[1,58,63], Y. Jiang[63], J.B. Jiao[50], Z. Jiao[24], S. Jin[43], Y. Jin[66], M.Q. Jing[1,63], T. Johansson[75], X. Kui[1], S. Kabana[34], N. Kalantar-Nayestanaki[64], X.L. Kang[10], X.S. Kang[41], R. Kappert[64], M. Kavatsyuk[64], B.C. Ke[81], A. Khoukaz[68], R. Kiuchi[1], R. Kliemt[14], O.B. Kolcu[62A], B. Kopf[4], M. Kuessner[4], A. Kupsc[45,75], W. Kühn[38], J.J. Lane[67], P. Larin[19], A. Lavania[27], L. Lavezzi[74A,74C], T.T. Lei[71,k], Z.H. Lei[71,58], H. Leithoff[36], M. Lellmann[36], T. Lenz[36], C. Li[48], C. Li[44], C.H. Li[40], Cheng Li[71,58], D.M. Li[81], F. Li[1,58], G. Li[1], H. Li[71,58], H.B. Li[1,63], H.J. Li[20], H.N. Li[56,i], Hui Li[44], J.R. Li[61], J.S. Li[59], J.W. Li[50], K.L. Li[20], Ke Li[1], L.J. Li[1,63], L.K. Li[1], Lei Li[3], M.H. Li[44], P.R. Li[39,j,k], Q.X. Li[50], S.X. Li[13], T. Li[50], W.D. Li[1,63], W.G. Li[1], X.H. Li[71,58], X.L. Li[50], Xiaoyu Li[1,63], Y.G. Li[47,g], Z.J. Li[59], Z.X. Li[16], C. Liang[43], H. Liang[35], H. Liang[71,58], H. Liang[1,63], Y.F. Liang[54], Y.T. Liang[32,63], G.R. Liao[15], L.Z. Liao[50], Y.P. Liao[1,63], J. Libby[27], A. Limphirat[60], D.X. Lin[32,63], T. Lin[1], B.J. Liu[1], B.X. Liu[76], C. Liu[35], C.X. Liu[1], F.H. Liu[53], Fang Liu[1], Feng Liu[7], G.M. Liu[56,i], H. Liu[39,j,k], H.B. Liu[16], H.M. Liu[1,63], Huanhuan Liu[1], Huihui Liu[22], J.B. Liu[71,58], J.L. Liu[72], J.Y. Liu[1,63], K. Liu[1], K.Y. Liu[41], Ke Liu[23], L. Liu[71,58], L.C. Liu[44], Lu Liu[44], M.H. Liu[13,f], P.L. Liu[1], Q. Liu[63], S.B. Liu[71,58], T. Liu[13,f], W.K. Liu[44], W.M. Liu[71,58], X. Liu[39,j,k], Y. Liu[81], Y. Liu[39,j,k], Y.B. Liu[44], Z.A. Liu[1,58,63], Z.Q. Liu[50], X.C. Lou[1,58,63], F.X. Lu[59], H.J. Lu[24], J.G. Lu[1,58], X.L. Lu[1], Y. Lu[8], Y.P. Lu[1,58], Z.H. Lu[1,63], C.L. Luo[42], M.X. Luo[80], T. Luo[13,f], X.L. Luo[1,58], X.R. Lyu[63], Y.F. Lyu[44], F.C. Ma[41], H.L. Ma[1], J.L. Ma[1,63], L.L. Ma[50], M.M. Ma[1,63], Q.M. Ma[1], R.Q. Ma[1,63], R.T. Ma[63], X.Y. Ma[1,58], Y. Ma[47,g], Y.M. Ma[32], F.E. Maas[19],

M. Maggiora[74A,74C], S. Malde[69], Q.A. Malik[73], A. Mangoni[29B], Y.J. Mao[47,g], Z.P. Mao[1],
S. Marcello[74A,74C], Z.X. Meng[66], J.G. Messchendorp[14,64], G. Mezzadri[30A], H. Miao[1,63], T.J. Min[43],
R.E. Mitchell[28], X.H. Mo[1,58,63], N.Yu. Muchnoi[5,b], J. Muskalla[36], Y. Nefedov[37], F. Nerling[19,d],
I.B. Nikolaev[5,b], Z. Ning[1,58], S. Nisar[12,l], Y. Niu[50], S.L. Olsen[63], Q. Ouyang[1,58,63], S. Pacetti[29B,29C],
X. Pan[55], Y. Pan[57], A. Pathak[35], P. Patteri[29A], Y.P. Pei[71,58], M. Pelizaeus[4], H.P. Peng[71,58],
K. Peters[14,d], J.L. Ping[42], R.G. Ping[1,63], S. Plura[36], S. Pogodin[37], V. Prasad[34], F.Z. Qi[1], H. Qi[71,58],
H.R. Qi[61], M. Qi[43], T.Y. Qi[13,f], S. Qian[1,58], W.B. Qian[63], C.F. Qiao[63], J.J. Qin[72], L.Q. Qin[15],
X.P. Qin[13,f], X.S. Qin[50], Z.H. Qin[1,58], J.F. Qiu[1], S.Q. Qu[61], C.F. Redmer[36], K.J. Ren[40],
A. Rivetti[74C], V. Rodin[64], M. Rolo[74C], G. Rong[1,63], Ch. Rosner[19], S.N. Ruan[44], N. Salone[45],
A. Sarantsev[37,c], Y. Schelhaas[36], K. Schoenning[75], M. Scodeggio[30A,30B], K.Y. Shan[13,f], W. Shan[25],
X.Y. Shan[71,58], J.F. Shangguan[55], L.G. Shao[1,63], M. Shao[71,58], C.P. Shen[13,f], H.F. Shen[1,63],
W.H. Shen[63], X.Y. Shen[1,63], B.A. Shi[63], H.C. Shi[71,58], J.L. Shi[13], J.Y. Shi[1], Q.Q. Shi[55], R.S. Shi[1,63],
X. Shi[1,58], J.J. Song[20], T.Z. Song[59], W.M. Song[35,1], Y.J. Song[13], Y.X. Song[47,g], S. Sosio[74A,74C],
S. Spataro[74A,74C], F. Stieler[36], Y.J. Su[63], G.B. Sun[76], G.X. Sun[1], H. Sun[63], H.K. Sun[1], J.F. Sun[20],
K. Sun[61], L. Sun[76], S.S. Sun[1,63], T. Sun[1,63], W.Y. Sun[35], Y. Sun[10], Y.J. Sun[71,58], Y.Z. Sun[1],
Z.T. Sun[50], Y.X. Tan[71,58], C.J. Tang[54], G.Y. Tang[1], J. Tang[59], Y.A. Tang[76], L.Y. Tao[72],
Q.T. Tao[26,h], M. Tat[69], J.X. Teng[71,58], V. Thoren[75], W.H. Tian[52], W.H. Tian[59], Y. Tian[32,63],
Z.F. Tian[76], I. Uman[62B], S.J. Wang[50], B. Wang[1], B.L. Wang[63], Bo Wang[71,58], C.W. Wang[43],
D.Y. Wang[47,g], F. Wang[72], H.J. Wang[39,j,k], H.P. Wang[1,63], J.P. Wang[50], K. Wang[1,58], L.L. Wang[1],
M. Wang[50], Meng Wang[1,63], S. Wang[13,f], S. Wang[39,j,k], T. Wang[13,f], T.J. Wang[44], W. Wang[59],
W. Wang[72], W.P. Wang[71,58], X. Wang[47,g], X.F. Wang[39,j,k], X.J. Wang[40], X.L. Wang[13,f], Y. Wang[61],
Y.D. Wang[46], Y.F. Wang[1,58,63], Y.H. Wang[48], Y.N. Wang[46], Y.Q. Wang[1], Yaqian Wang[18,1],
Yi Wang[61], Z. Wang[1,58], Z.L. Wang[72], Z.Y. Wang[1,63], Ziyi Wang[63], D. Wei[70], D.H. Wei[15],
F. Weidner[68], S.P. Wen[1], C.W. Wenzel[4], U. Wiedner[4], G. Wilkinson[69], M. Wolke[75], L. Wollenberg[4],
C. Wu[40], J.F. Wu[1,63], L.H. Wu[1], L.J. Wu[1,63], X. Wu[13,f], X.H. Wu[35], Y. Wu[71], Y.J. Wu[32], Z. Wu[1,58],
L. Xia[71,58], X.M. Xian[40], T. Xiang[47,g], D. Xiao[39,j,k], G.Y. Xiao[43], S.Y. Xiao[1], Y.L. Xiao[13,f],
Z.J. Xiao[42], C. Xie[43], X.H. Xie[47,g], Y. Xie[50], Y.G. Xie[1,58], Y.H. Xie[7], Z.P. Xie[71,58], T.Y. Xing[1,63],
C.F. Xu[1,63], C.J. Xu[59], G.F. Xu[1], H.Y. Xu[66], Q.J. Xu[17], Q.N. Xu[31], W. Xu[1,63], W.L. Xu[66],
X.P. Xu[55], Y.C. Xu[78], Z.P. Xu[43], Z.S. Xu[63], F. Yan[13,f], L. Yan[13,f], W.B. Yan[71,58], W.C. Yan[81],
X.Q. Yan[1], H.J. Yang[51,e], H.L. Yang[35], H.X. Yang[1], Tao Yang[1], Y. Yang[13,f], Y.F. Yang[44],
Y.X. Yang[1,63], Yifan Yang[1,63], Z.W. Yang[39,j,k], Z.P. Yao[50], M. Ye[1,58], M.H. Ye[9], J.H. Yin[1],
Z.Y. You[59], B.X. Yu[1,58,63], C.X. Yu[44], G. Yu[1,63], J.S. Yu[26,h], T. Yu[72], X.D. Yu[47,g], C.Z. Yuan[1,63],
L. Yuan[2], S.C. Yuan[1], X.Q. Yuan[1], Y. Yuan[1,63], Z.Y. Yuan[59], C.X. Yue[40], A.A. Zafar[73], F.R. Zeng[50],
X. Zeng[13,f], Y. Zeng[26,h], Y.J. Zeng[1,63], X.Y. Zhai[35], Y.C. Zhai[50], Y.H. Zhan[59], A.Q. Zhang[1,63],
B.L. Zhang[1,63], B.X. Zhang[1], D.H. Zhang[44], G.Y. Zhang[20], H. Zhang[71], H.H. Zhang[59], H.H. Zhang[35],
H.Q. Zhang[1,58,63], H.Y. Zhang[1,58], J.J. Zhang[52], J.L. Zhang[21], J.Q. Zhang[42], J.W. Zhang[1,58,63],
J.X. Zhang[39,j,k], J.Y. Zhang[1], J.Z. Zhang[1,63], Jianyu Zhang[63], Jiawei Zhang[1,63], L.M. Zhang[61],
L.Q. Zhang[59], Lei Zhang[43], P. Zhang[1], Q.Y. Zhang[40,81], Shuihan Zhang[1,63], Shulei Zhang[26,h],
X.D. Zhang[46], X.M. Zhang[1], X.Y. Zhang[50], Xuyan Zhang[55], Y. Zhang[72], Y. Zhang[69], Y.T. Zhang[81],
Y.H. Zhang[1,58], Yan Zhang[71,58], Yao Zhang[1], Z.H. Zhang[1], Z.L. Zhang[35], Z.Y. Zhang[76],
Z.Y. Zhang[44], G. Zhao[1], J. Zhao[40], J.Y. Zhao[1,63], J.Z. Zhao[1,58], Lei Zhao[71,58], Ling Zhao[1],
M.G. Zhao[44], S.J. Zhao[81], Y.B. Zhao[1,58], Y.X. Zhao[32,63], Z.G. Zhao[71,58], A. Zhemchugov[37,a],
B. Zheng[72], J.P. Zheng[1,58], W.J. Zheng[1,63], Y.H. Zheng[63], B. Zhong[42], X. Zhong[59], H. Zhou[50],

L.P. Zhou[1,63], X. Zhou[76], X.K. Zhou[7], X.R. Zhou[71,58], X.Y. Zhou[40], Y.Z. Zhou[13,f], J. Zhu[44], K. Zhu[1], K.J. Zhu[1,58,63], L. Zhu[35], L.X. Zhu[63], S.H. Zhu[70], S.Q. Zhu[43], T.J. Zhu[13,f], W.J. Zhu[13,f], Y.C. Zhu[71,58], Z.A. Zhu[1,63], J.H. Zou[1], J. Zu[71,58]

[1] *Institute of High Energy Physics, Beijing 100049, People's Republic of China*

[2] *Beihang University, Beijing 100191, People's Republic of China*

[3] *Beijing Institute of Petrochemical Technology, Beijing 102617, People's Republic of China*

[4] *Bochum Ruhr-University, D-44780 Bochum, Germany*

[5] *Budker Institute of Nuclear Physics SB RAS (BINP), Novosibirsk 630090, Russia*

[6] *Carnegie Mellon University, Pittsburgh, Pennsylvania 15213, USA*

[7] *Central China Normal University, Wuhan 430079, People's Republic of China*

[8] *Central South University, Changsha 410083, People's Republic of China*

[9] *China Center of Advanced Science and Technology, Beijing 100190, People's Republic of China*

[10] *China University of Geosciences, Wuhan 430074, People's Republic of China*

[11] *Chung-Ang University, Seoul, 06974, Republic of Korea*

[12] *COMSATS University Islamabad, Lahore Campus, Defence Road, Off Raiwind Road, 54000 Lahore, Pakistan*

[13] *Fudan University, Shanghai 200433, People's Republic of China*

[14] *GSI Helmholtzcentre for Heavy Ion Research GmbH, D-64291 Darmstadt, Germany*

[15] *Guangxi Normal University, Guilin 541004, People's Republic of China*

[16] *Guangxi University, Nanning 530004, People's Republic of China*

[17] *Hangzhou Normal University, Hangzhou 310036, People's Republic of China*

[18] *Hebei University, Baoding 071002, People's Republic of China*

[19] *Helmholtz Institute Mainz, Staudinger Weg 18, D-55099 Mainz, Germany*

[20] *Henan Normal University, Xinxiang 453007, People's Republic of China*

[21] *Henan University, Kaifeng 475004, People's Republic of China*

[22] *Henan University of Science and Technology, Luoyang 471003, People's Republic of China*

[23] *Henan University of Technology, Zhengzhou 450001, People's Republic of China*

[24] *Huangshan College, Huangshan 245000, People's Republic of China*

[25] *Hunan Normal University, Changsha 410081, People's Republic of China*

[26] *Hunan University, Changsha 410082, People's Republic of China*

[27] *Indian Institute of Technology Madras, Chennai 600036, India*

[28] *Indiana University, Bloomington, Indiana 47405, USA*

[29] *INFN Laboratori Nazionali di Frascati , (A)INFN Laboratori Nazionali di Frascati, I-00044, Frascati, Italy; (B)INFN Sezione di Perugia, I-06100, Perugia, Italy; (C)University of Perugia, I-06100, Perugia, Italy*

[30] *INFN Sezione di Ferrara, (A)INFN Sezione di Ferrara, I-44122, Ferrara, Italy; (B)University of Ferrara, I-44122, Ferrara, Italy*

[31] *Inner Mongolia University, Hohhot 010021, People's Republic of China*

[32] *Institute of Modern Physics, Lanzhou 730000, People's Republic of China*

[33] *Institute of Physics and Technology, Peace Avenue 54B, Ulaanbaatar 13330, Mongolia*

[34] *Instituto de Alta Investigación, Universidad de Tarapacá, Casilla 7D, Arica 1000000, Chile*

[35] *Jilin University, Changchun 130012, People's Republic of China*

[36] *Johannes Gutenberg University of Mainz, Johann-Joachim-Becher-Weg 45, D-55099 Mainz, Germany*

[37] *Joint Institute for Nuclear Research, 141980 Dubna, Moscow region, Russia*

[38] *Justus-Liebig-Universitaet Giessen, II. Physikalisches Institut, Heinrich-Buff-Ring 16, D-35392 Giessen, Germany*

[39] *Lanzhou University, Lanzhou 730000, People's Republic of China*

[40] *Liaoning Normal University, Dalian 116029, People's Republic of China*

[41] *Liaoning University, Shenyang 110036, People's Republic of China*

[42] *Nanjing Normal University, Nanjing 210023, People's Republic of China*

[43] *Nanjing University, Nanjing 210093, People's Republic of China*

[44] *Nankai University, Tianjin 300071, People's Republic of China*

[45] *National Centre for Nuclear Research, Warsaw 02-093, Poland*

[46] *North China Electric Power University, Beijing 102206, People's Republic of China*

[47] *Peking University, Beijing 100871, People's Republic of China*

[48] *Qufu Normal University, Qufu 273165, People's Republic of China*

[49] *Shandong Normal University, Jinan 250014, People's Republic of China*

[50] *Shandong University, Jinan 250100, People's Republic of China*

[51] *Shanghai Jiao Tong University, Shanghai 200240, People's Republic of China*

[52] *Shanxi Normal University, Linfen 041004, People's Republic of China*

[53] *Shanxi University, Taiyuan 030006, People's Republic of China*

[54] *Sichuan University, Chengdu 610064, People's Republic of China*

[55] *Soochow University, Suzhou 215006, People's Republic of China*

[56] *South China Normal University, Guangzhou 510006, People's Republic of China*

[57] *Southeast University, Nanjing 211100, People's Republic of China*

[58] *State Key Laboratory of Particle Detection and Electronics, Beijing 100049, Hefei 230026, People's Republic of China*

[59] *Sun Yat-Sen University, Guangzhou 510275, People's Republic of China*

[60] *Suranaree University of Technology, University Avenue 111, Nakhon Ratchasima 30000, Thailand*

[61] *Tsinghua University, Beijing 100084, People's Republic of China*

[62] *Turkish Accelerator Center Particle Factory Group, (A)Istinye University, 34010, Istanbul, Turkey; (B)Near East University, Nicosia, North Cyprus, 99138, Mersin 10, Turkey*

[63] *University of Chinese Academy of Sciences, Beijing 100049, People's Republic of China*

[64] *University of Groningen, NL-9747 AA Groningen, The Netherlands*

[65] *University of Hawaii, Honolulu, Hawaii 96822, USA*

[66] *University of Jinan, Jinan 250022, People's Republic of China*

[67] *University of Manchester, Oxford Road, Manchester, M13 9PL, United Kingdom*

[68] *University of Muenster, Wilhelm-Klemm-Strasse 9, 48149 Muenster, Germany*

[69] *University of Oxford, Keble Road, Oxford OX13RH, United Kingdom*

[70] *University of Science and Technology Liaoning, Anshan 114051, People's Republic of China*

[71] *University of Science and Technology of China, Hefei 230026, People's Republic of China*

[72] *University of South China, Hengyang 421001, People's Republic of China*

[73] *University of the Punjab, Lahore-54590, Pakistan*

[74] *University of Turin and INFN, (A)University of Turin, I-10125, Turin, Italy; (B)University of Eastern Piedmont, I-15121, Alessandria, Italy; (C)INFN, I-10125, Turin, Italy*

[75] *Uppsala University, Box 516, SE-75120 Uppsala, Sweden*

[76] *Wuhan University, Wuhan 430072, People's Republic of China*

[77] *Xinyang Normal University, Xinyang 464000, People's Republic of China*

[78] *Yantai University, Yantai 264005, People's Republic of China*

[79] *Yunnan University, Kunming 650500, People's Republic of China*

[80] *Zhejiang University, Hangzhou 310027, People's Republic of China*

[81] *Zhengzhou University, Zhengzhou 450001, People's Republic of China*

[a] *Also at the Moscow Institute of Physics and Technology, Moscow 141700, Russia*

[b] *Also at the Novosibirsk State University, Novosibirsk, 630090, Russia*

[c] *Also at the NRC "Kurchatov Institute", PNPI, 188300, Gatchina, Russia*

[d] *Also at Goethe University Frankfurt, 60323 Frankfurt am Main, Germany*

[e] *Also at Key Laboratory for Particle Physics, Astrophysics and Cosmology, Ministry of Education; Shanghai Key Laboratory for Particle Physics and Cosmology; Institute of Nuclear and Particle Physics, Shanghai 200240, People's Republic of China*

[f] *Also at Key Laboratory of Nuclear Physics and Ion-beam Application (MOE) and Institute of Modern Physics, Fudan University, Shanghai 200443, People's Republic of China*

[g] *Also at State Key Laboratory of Nuclear Physics and Technology, Peking University, Beijing 100871, People's Republic of China*

[h] *Also at School of Physics and Electronics, Hunan University, Changsha 410082, China*

[i] *Also at Guangdong Provincial Key Laboratory of Nuclear Science, Institute of Quantum Matter, South China Normal University, Guangzhou 510006, China*

[j] *Also at Frontiers Science Center for Rare Isotopes, Lanzhou University, Lanzhou 730000, People's Republic of China*

[k] *Also at Lanzhou Center for Theoretical Physics, Lanzhou University, Lanzhou 730000, People's Republic of China*

[l] *Also at the Department of Mathematical Sciences, IBA, Karachi 75270, Pakistan*